JIDC | THE JOURNAL OF INFECTION IN DEVELOPING COUNTRIES

Original Article

Integrative analysis of miRNA-RBP-splicing interactions during respiratory syncytial virus infection

Mingzhen Cheng[1], Hongtao Xu[1], Fang Yuan[1], Shuangshuang Li[1]

[1] Department of Pediatrics, Chinese PLA General Hospital of Central Theater Command, Wuhan 430070, Hubei Province, China

Abstract

Introduction: Respiratory syncytial virus (RSV) is a major cause of severe acute lower respiratory tract infections (ALRI), with incomplete elucidation of its pathogenesis and intricate host-virus crosstalk constraining the development of effective therapies. The post-transcriptional interplay among microRNAs (miRNAs), RNA-binding proteins (RBPs), and alternative splicing (AS) is a critical, yet underexplored host response layer.

Methodology: We integrated and analyzed three public datasets (GSE231784, GSE231788, and GSE155151) of RSV-infected A549 cells, screened differentially expressed miRNAs, identified conserved differentially expressed RBPs, used SUVA to detect AS events, and constructed a miRNA-RBP-AS network to find core axis. This integrated bioinformatics approach enabled systematic dissection of multi-layered post-transcriptional regulation during RSV infection.

Results: Our analysis revealed that RSV infection substantially alters host post-transcriptional regulation, with 86 conserved differentially expressed RBPs and 94 conserved AS events identified. A potential miRNA-RBP-AS axis was uncovered via regulatory network construction. Crucially, this axis suggests that the downregulation of let-7 family miRNAs (e.g., let-7f-2-3p, let-7a-3p) is strongly associated with the upregulation of the RBP genes *SAMD4A* and *ENOX1*. The expression of these RBPs, in turn, correlates with the AS of host genes that are implicated in viral replication and immunity, such as *TNIP1* and *NR5A2*.

Conclusions: These findings propose that RSV may exploit this post-transcriptional crosstalk to modulate host immunity and facilitate viral replication. Through bioinformatics analysis, this study provides a novel, system-level map of RSV-host interactions and identifies the let-7-*SAMD4A/ENOX1-TNIP1/NR5A2* axis as a promising new target for future antiviral strategies, though this requires further experimental validation.

Key words: RSV; AS; RBP; microRNA.

J Infect Dev Ctries 2026; 20(7):962-973. doi:10.3855/jidc.22201

(Received 08 August 2025 – Accepted 06 December 2025)

Introduction

Respiratory syncytial virus (RSV) remains a leading global pathogen responsible for severe acute lower respiratory tract infections (ALRI) [1], and its pathogenesis involves dynamic interactions between viral replication and host immune responses within infected cells [2,3]. A thorough elucidation of the host's response mechanisms to RSV infection is crucial for interpreting its pathophysiology and identifying novel targets for effective antiviral interventions.

RNA-binding proteins (RBPs) are core molecules that regulate alternative splicing (AS). By binding to specific sequences on precursor mRNA (pre-mRNA), they determine the assembly of the spliceosome and the selection of splice sites, thereby generating multiple mRNA isoforms from a single gene and ultimately expanding proteomic diversity [4]. Meanwhile, RBPs are central to the host's post-transcriptional response to RNA viruses [5]. Viruses often hijack RBPs to facilitate their replication, while the host uses RBPs as antiviral sensors and effectors [6]. Viral manipulation of RBP activity induces widespread dysregulation of host cell splicing [7,8], with profound implications for pathogenesis—altered splicing of host transcripts modulates antiviral immunity and cellular susceptibility to infection [9]. For example, RSV infection regulates the splicing of key immune factors like IKKγ [10] and relies on specific RBPs such as G3BP1 to promote viral replication [11].

In addition to RBPs and AS, microRNAs (miRNAs) form another key layer of post-transcriptional control in host cells. miRNAs are small non-coding RNAs that repress gene expression by targeting mRNAs [12]. Similar to RBPs, the cellular miRNA landscape is significantly altered during RSV infection [13]. Some of these RSV-induced miRNA changes help restrict viral replication, while others are co-opted by RSV to enhance its own propagation (e.g., the suppression of miR-24) [14]. Despite growing evidence for the individual roles of RBPs, AS, and miRNAs in the host

response to RSV, the synergistic crosstalk and coordinated regulation between these three post-transcriptional pillars remain largely unstudied.

This study was designed to systematically dissect the crosstalk among these post-transcriptional regulatory layers. We aimed to construct a comprehensive miRNA-RBP-AS regulatory network active during RSV infection by performing an integrative bioinformatic analysis of public miRNA-seq and RNA-seq datasets. This systems-level approach enables the identification of key molecular nodes and pathways rewired by the virus, providing a new framework for understanding RSV pathogenesis and uncovering potential vulnerabilities for future antiviral therapies.

Methodology

Data acquisition and pre-processing

Three public datasets from the Gene Expression Omnibus (GEO) were selected based on their experimental consistency to construct a robust and comprehensive map of post-transcriptional regulation. All chosen datasets utilized the human alveolar adenocarcinoma cell line (A549), a standard and widely used model for in vitro RSV research. Specifically, the analysis included: (1) a miRNA-seq dataset (GSE231784) from A549 cells infected with RSV strain A2 for 48 hours; (2) a corresponding RNA-seq dataset (GSE231788) from the same experimental conditions (A549 cells, RSV-A2, 48 hours infection); (3) and a time-course RNA-seq dataset (GSE155151) of A549 cells infected with RSV for 24 and 48 hours. This combination of datasets, with its consistent cell line model and overlapping time points, enabled a cross-validated analysis to identify conserved host responses. The raw FASTQ sequencing data were downloaded from the Sequence Read Archive (SRA) and then processed with fastp (version 0.23.4) [15] to remove adapter sequences, low-quality reads, and other technical artifacts under default settings.

Read alignment and quantification

In the case of RNA-seq data, clean reads were aligned to the human reference genome (GRCh38) using the STAR aligner (v2.7.10b) with modified parameters: "--outFilterMismatchNoverReadLmax 0.04 --outFilterMismatchNmax 999 --alignIntronMax 500000 --alignMatesGapMax 1000000 --alignSJDBoverhangMin 8 --outFilterMatchNminOverLread 0.33 --outFilterScoreMinOverLread 0.33 --outSAMstrandField intronMotif --twopassMode Basic --outSAMmultNmax 2 --alignSJoverhangMin 8 --outFilterType BySJout --outSJfilterReads Unique --alignEndsType EndToEnd". Gene expression was quantified using only uniquely mapped reads. Raw integer counts were calculated for each gene and used as the direct input for downstream differential expression analysis. These raw counts were normalized to reads per kilobase of exon per million mapped fragments (FPKM) to adjust for variations in gene length and sequencing depth for data visualization and correlation analysis. In the case of miRNA-seq data, reads were aligned to the human miRNA database (miRBase v22) using bowtie (v1.3.1) to obtain miRNA expression counts. The raw count matrices were used for differential expression analysis. Additionally, transcripts per million (TPM) values were calculated for data visualization and network correlation analysis to normalize for sequencing depth and transcript length.

Differential expression analysis

Differential expression analysis of genes between RSV-infected and mock-infected samples was performed using the DESeq2 R package (v1.46.0) [16]. Genes with a Benjamini-Hochberg adjusted p value (FDR) ≤ 0.05 and a fold change (FC) ≥ 1.5 (for upregulation) or ≤ 0.66 (for downregulation) were considered significantly differentially expressed. This combined threshold was selected to ensure statistical rigor while capturing biologically substantial expression changes. A comprehensive list of 2,141 human RBPs, compiled from previous landmark studies [17–20], was used to filter and identify differentially expressed RBPs from the gene list. In the case of miRNAs, differential expression analysis was conducted using the edgeR R package (v4.4.1), which identified a total of 176 significantly altered miRNAs. Significance was determined based on an FDR threshold of ≤ 0.05 and a fold change of ≥ 1.5 or ≤ 0.66, indicating upregulation or downregulation, respectively.

Alternative splicing analysis

AS events were identified and quantified from the RNA-seq alignment files (BAM files) using the SUVA pipeline [21]. This method defines four types of AS events: alternative 3' splice site (alt3p)—two splice junctions (SJs) share a common 5' splice site with alternative 3' splice sites; alternative 5' splice site (alt5p)—two SJs share a common 3' splice site with alternative 5' splice sites; overlapped (olp)—SJs have no shared splice sites but partially overlapping splicing regions; contained (contain)—one complete SJ is

entirely nested within the genomic range of another longer SJ.

The splicing ratio difference between sample groups and the proportion of reads supporting a specific splicing event relative to all reads covering that event region (pSAR) were calculated for each event. To identify robust splicing changes, regulated alternative splicing (RAS) events were defined as those exhibiting a dominant isoform switch (|splicing ratio difference| ≥ 0.15), filtered by a pSAR threshold of ≥ 50%.

Prediction of miRNA targets

miRNA target prediction was performed using the multiMiR R package (v3.21), integrating results from a total of 9 databases, including both predicted and experimentally validated sources (miRecords [22], miRTarBase [23] and TarBase [24]) and validation (miRDB [25], DIANA-microT [26], miRanda [27], PicTar [28], TargetScan [29], PITA [30], EIMMo [31], and MicroCosm Targets [32]). miRNA-target gene interactions supported by at least 3 of these databases were considered high-confidence and retained for downstream analyses.

Construction of the miRNA-RBP-AS regulatory network

A co-expression analysis was performed to link the expression of differentially expressed RBPs with the splicing ratios of RAS events. The Spearman correlation coefficient (r) was calculated for each RBP-RAS pair across all samples. We performed a sensitivity analysis by evaluating correlation thresholds from 0.6 to 0.98 to balance network coverage with interaction reliability. Only pairs with a Spearman's |r| ≥ 0.9 and a p value ≤ 0.01 were retained to construct a high-confidence regulatory network. Finally, the predicted miRNA-RBP interactions were integrated with the RBP-RAS network to form the final miRNA-RBP-AS regulatory map.

Functional enrichment analysis

To identify functional categories of genes, we employed the clusterProfiler package (v4.6.2) [33], which enabled us to determine Gene Ontology (GO) terms and Kyoto Encyclopedia of Genes and Genomes (KEGG) pathways, using all annotated human genes as the background set. Significantly enriched terms were identified based on a p adjust value < 0.05.

Other analysis

Principal component analysis (PCA) was conducted using the factoextra R package [34] to visualize sample clustering. Heatmaps were generated using the pheatmap R package [35] with Euclidean distance for clustering.

Results

RSV infection profoundly remodels the host miRNA landscape

We profiled miRNA expression in A549 cells at 48 hours post-RSV infection (hpi) (GSE231784) to delineate RSV's impact on host post-transcriptional regulation. PCA revealed a clear and distinct separation between the RSV-infected and mock-infected control groups, indicating a profound and consistent alteration of the host miRNA landscape following infection (Figure 1A). Differential expression analysis identified 176 significantly altered miRNAs (101 upregulated, 75 downregulated; Figure 1B), with notable downregulation of conserved let-7 family members (Figure 1C). In order to explore functional consequences, we predicted target genes of dysregulated miRNAs using an integrative approach requiring validation from ≥ 3 databases, identifying 9,479 high-confidence targets (Figure 1D). Functional enrichment analysis revealed GO enrichment in small GTPase-mediated signal transduction and Wnt signaling, while KEGG analysis supported enrichment in mitogen-activated protein kinase (MAPK), Wnt, and TGF-β pathways (Figure 1E). Collectively, RSV infection induces significant remodeling of the host miRNA profile, predicted to impact key signaling pathways—particularly Wnt signaling, critical for cellular homeostasis and immune responses.

RSV infection triggers a dynamic reprogramming of host RNA-binding proteins

We analyzed two RNA-seq datasets to investigate whether RSV infection alters the expression of RNA fate master regulators (RBPs). In the case of dataset GSE231788, we compared RSV-infected A549 cells with mock-infected controls at 24 hours, and identified 3,761 upregulated and 1,300 downregulated differentially expressed genes (DEGs) (Supplementary Figure 1A–B). In the case of GSE155151, comparisons with uninfected controls detected 1,855 DEGs at 24 hpi, 4,185 DEGs at 48 hpi, and 1,252 DEGs between 48 hpi and 24 hpi; we further selected DEGs common to the three comparisons (24 hpi vs. control, 48 hpi vs. control, 48 hpi vs. 24 hpi) with consistent expression trends across 2 or 3 groups as time-responsive host genes, identifying 4,485 such specific DEGs (Supplementary Figure 1B–C). The intersection of DEGs from GSE231788 and GSE155151 yielded 1,823

conserved DEGs (Supplementary Figure 1C). The Gene Ontology-Biological Process (GO-BP) enrichment analysis showed that the up-regulated DEGs were mainly enriched in pathways such as response to virus, bacterial-derived molecules, and lipopolysaccharide; while the down-regulated DEGs were mainly enriched in pathways such as nucleosome assembly and protein-DNA complex assembly (Supplementary Figure 1D).

After integrating the two datasets, we identified 86 conserved, differentially expressed RBPs, comprising

Figure 1. Differential expression analysis of microRNAs (miRNAs) and target gene prediction.

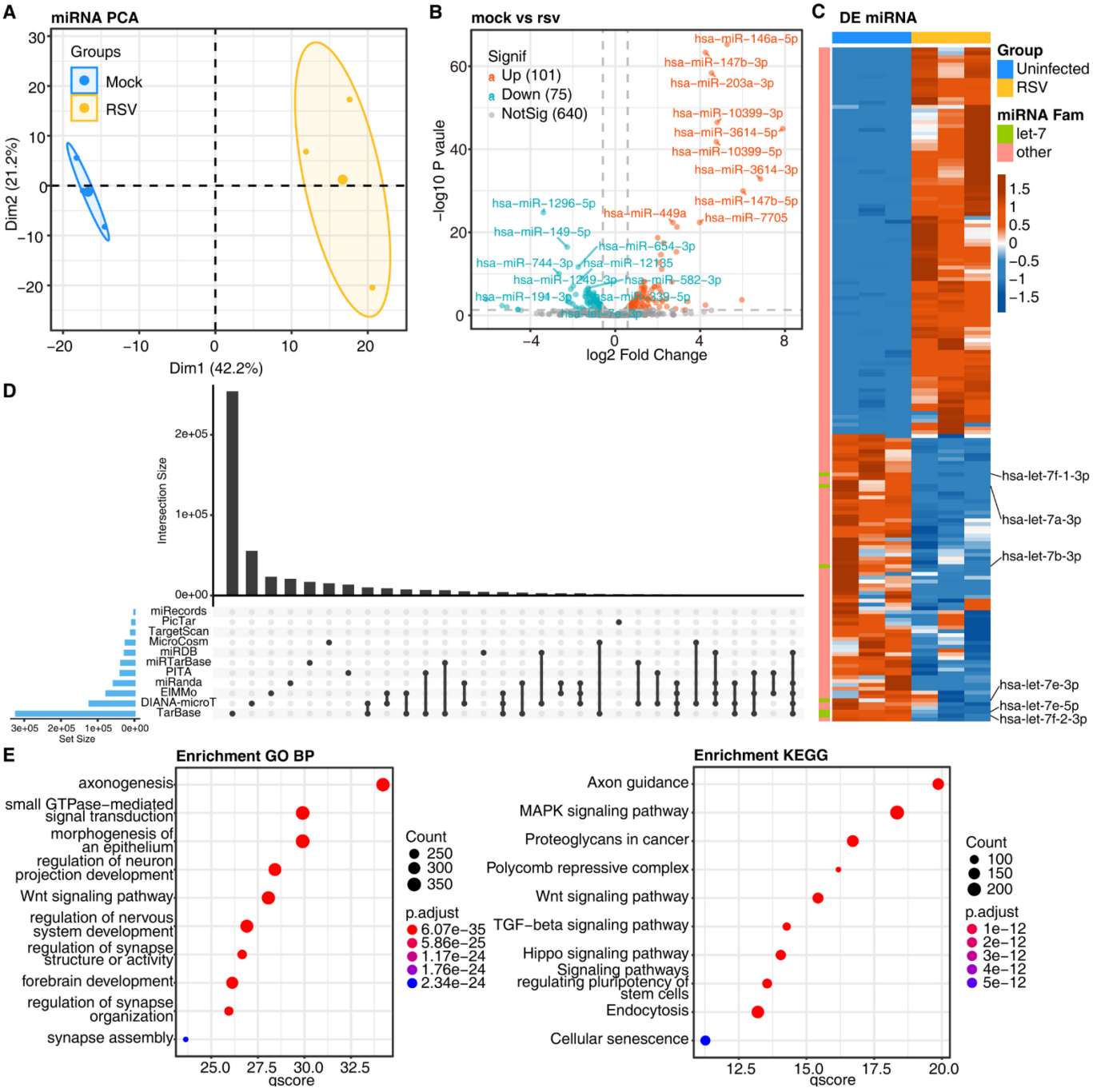

A. Principal component analysis (PCA) of miRNA expression levels; **B.** Volcano plot displaying differentially expressed miRNAs (identified using DESeq2; FoldChange ≥ 1.5 or FoldChange ≤ 0.66, FDR ≤ 0.05); **C.** Heatmap showing the Z-score normalized expression levels of differentially expressed miRNAs; **D.** UpSet plot illustrating the predicted target genes of the identified miRNAs. miRNA-target gene pairs supported by at least three databases were selected for downstream analysis; **E.** The Gene Ontology-Biological Process (GO-BP) and Kyoto Encyclopedia of Genes and Genomes (KEGG) enrichment analyses of the predicted target genes of differentially expressed miRNAs.

59 that were significantly upregulated and 27 that were downregulated following RSV infection (Figure 2A–B). GO enrichment analysis showed that upregulated RBPs were significantly enriched in antiviral pathways, including "defense response to virus," "negative regulation of viral replication," and "regulation of viral life cycle"; while downregulated RBPs were enriched in core cellular processes such as "mitochondrial translation" and "spliceosomal snRNP assembly"—suggesting a virus-induced suppression of core RNA and protein synthesis machinery (Figure 2C). Notably, the upregulated RBP group included antiviral interferon-stimulated genes (ISGs: *IFI16*, *IFIT1*, *IFIT5*, *ISG20*), and time-course analysis (from GSE155151) confirmed their progressive expression increase from 24 to 48 hpi, reflecting a dynamic, strengthened host antiviral response and reprogramming of post-transcriptional machinery (Figure 2D).

RSV infection systematically rewires the host alternative splicing program

Given the RSV-induced reprogramming of host RBPs—key regulators of AS—we investigated whether infection alters the host splicing landscape. PCA of AS events showed distinct clustering of RSV-infected vs. mock-infected cells, confirming profound changes in the cellular splicing program (Figure 3A). Characterization of AS events in GSE231788 (via SUVA pipeline) identified thousands of events, with alternative 5' splice site (alt5p) and intron containment (contain) as the most abundant types (Figure 3B); canonical classification revealed cassette exons and exon skipping as the most frequent changes (Figure 3C). This dataset alone contained 821 dominant

Figure 2. Differential expression and functional analysis of RNA-binding proteins (RBPs).

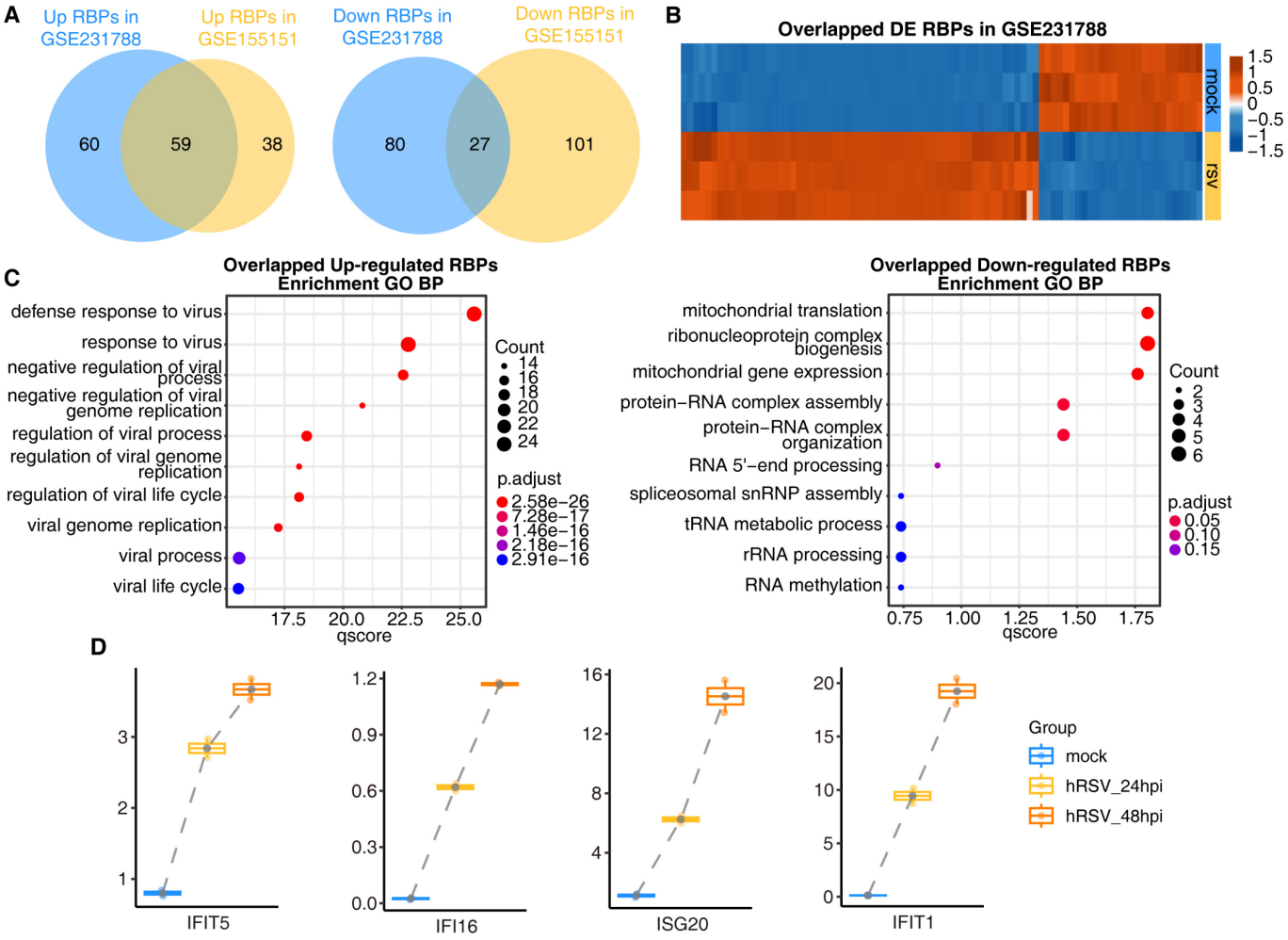

A. Venn diagram showing the commonly dysregulated RBPs shared between the GSE231788 and GSE155151 datasets; **B.** Heatmap displaying the expression levels of the commonly dysregulated RBPs in the GSE231788 dataset; **C.** GO enrichment analysis of the conserved differentially expressed RBPs; **D.** Expression profiles of IFIT5, IFI16, ISG20, and IFIT1 in the GSE155151 dataset.

Figure 3. Alternative splicing (AS) analysis in the GSE231788 dataset.

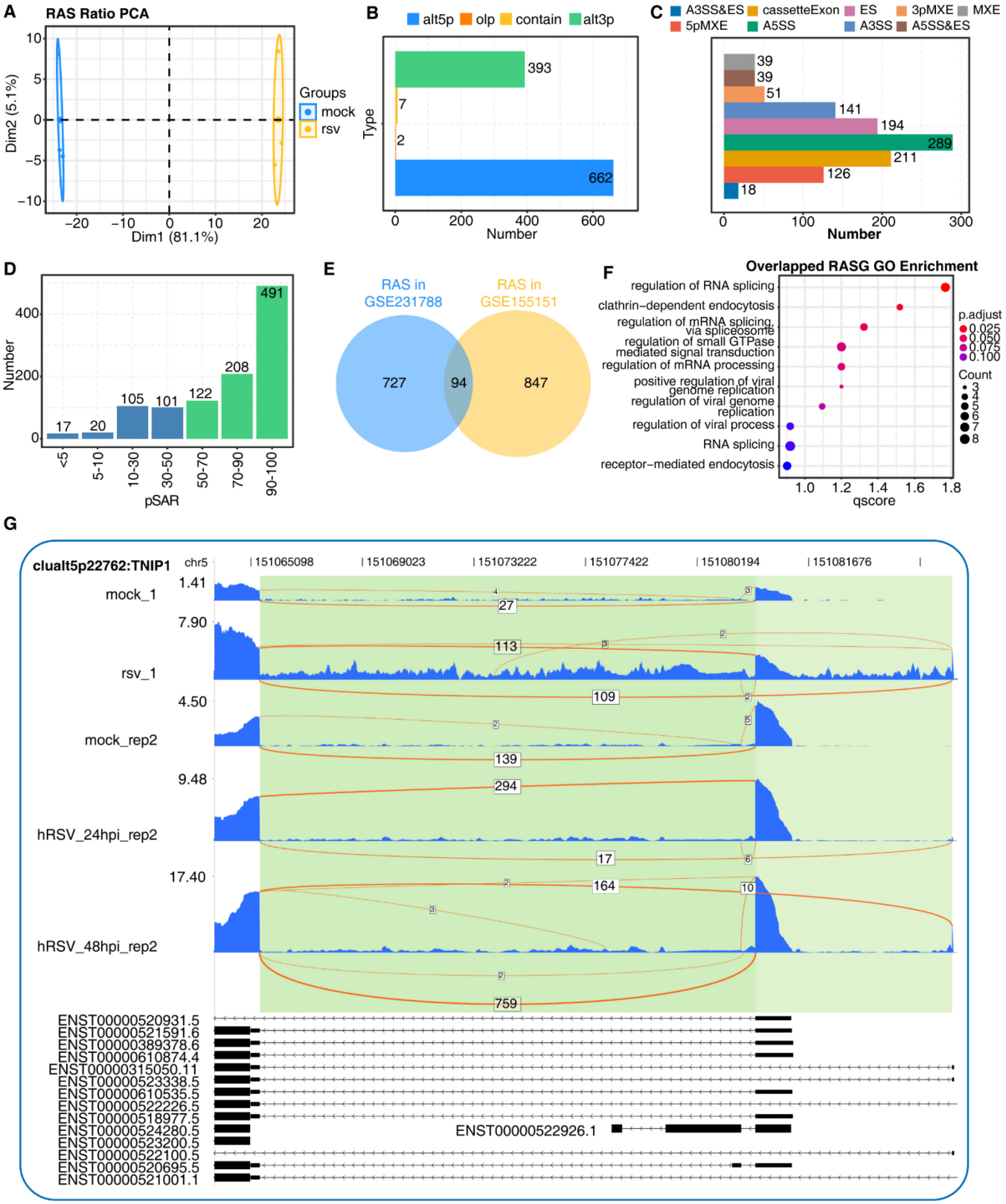

A. PCA based on the proportions of AS events; **B.** Number of AS events identified in the GSE231788 dataset using the SUVA algorithm; **C.** Number of SUVA-detected AS events in GSE231788 that were annotated to canonical AS event types; **D.** Bar plot showing the distribution of proportion of SUVA AS events ratio (pSAR); AS events with pSAR > 50% were selected for downstream analysis; **E.** Venn diagram indicating the number of conserved SUVA AS events shared between the two datasets; **F.** GO enrichment analysis of host genes corresponding to the conserved AS events; **G.** Read distribution and quantification of the AS event clualt5p22762 in the TNIP1 gene, illustrating the differential inclusion of splice variants.

differential AS events, reflecting RSV's widespread impact on host splicing (Figure 3D). In order to identify conserved, reproducible splicing dysregulation, we integrated the findings with GSE155151 (time-course dataset) and uncovered 94 high-confidence RAS events conserved across both systems (Figure 3E, Supplementary Figure 2A–C), indicating targeted rather than random rewiring of the host splicing machinery by RSV. GO analysis of the 94 regulated alternative splicing genes (RASGs) showed significant enrichment in "regulation of RNA splicing," "regulation of mRNA processing," and—critically—"positive regulation of viral genome replication," suggesting RSV manipulates host gene splicing to support its life cycle (Figure 3F). The relevant genes included *TNIP1*, *NR5A2*, *ADAR*, and *SRPK2*, with splicing event distributions across sample groups detailed in figures (Figure 3G, Supplementary Figure 2D, Supplementary Figure 3A–B). A case study of *TNIP1* (a key viral replication-associated gene) revealed an infection-dependent splicing shift: RSV-infected cells showed a dramatic increase in selection

Figure 4. Co-expression regulatory network analysis of miRNAs, RBPs, and AS events.

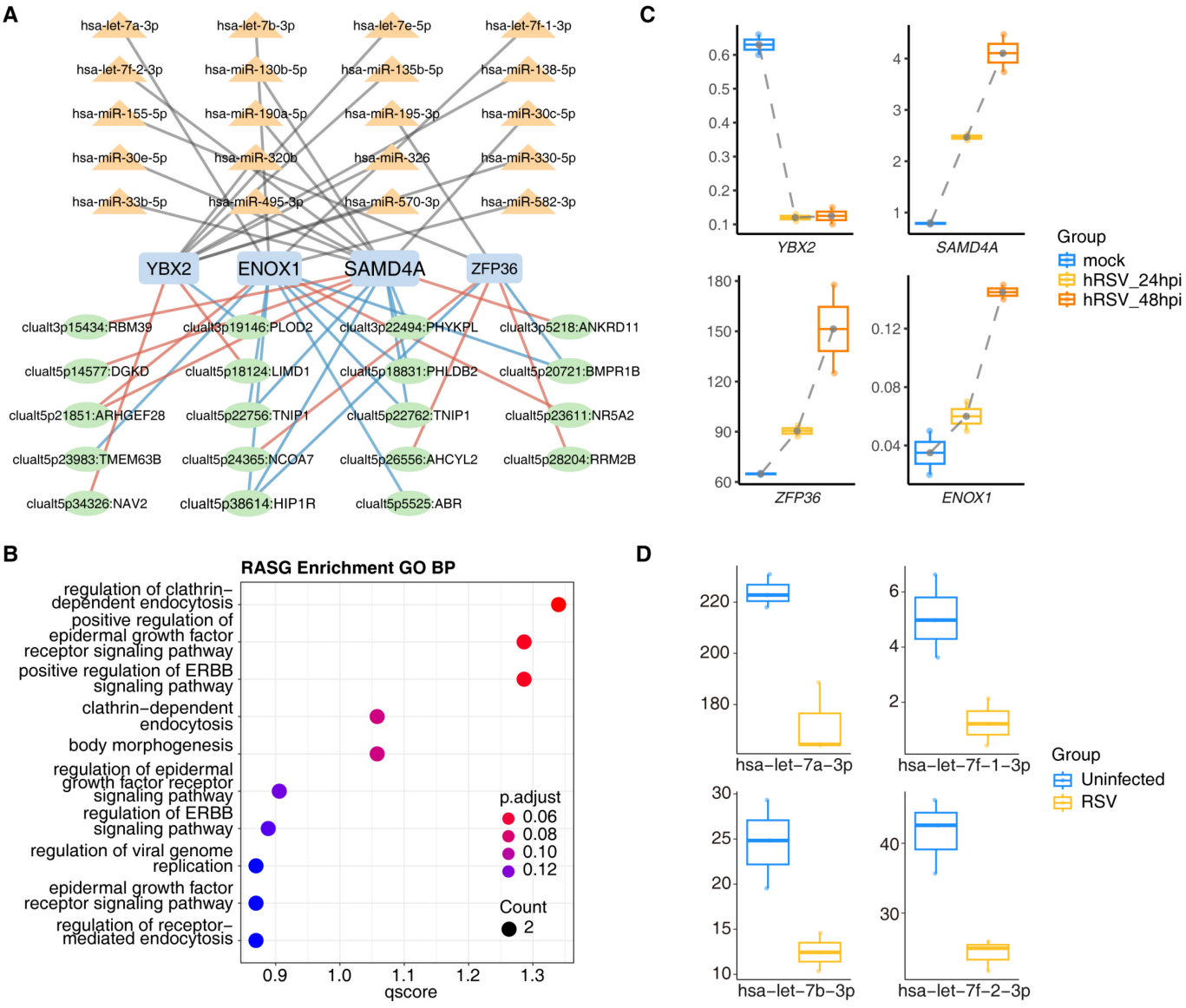

A. Co-expression regulatory network integrating miRNAs, RBPs, and AS events. Triangles represent miRNAs, rounded rectangles represent RBPs, and ellipses represent AS events. Red edges indicate positive correlations, and blue edges indicate negative correlations (RBP-AS ratio Spearman correlation, $|r| \geq 0.9$, $p \leq 0.01$); **B.** GO enrichment analysis of host genes corresponding to AS events in the network; **C.** Box plot showing the expression levels of network-associated RBPs in the GSE155151 dataset; group means are connected with dashed lines; **D.** Boxplots presenting the expression levels (TPM) of miRNAs let-7f-2-3p, let-7f-1-3p, let-7a-3p, and let-7b-3p that target the RBPs SAMD4A and ENOX1.

of the distal, shorter exon compared to mock controls (Figure 3G), illustrating how RSV hijacks the host splicing program to create a replication-favorable cellular environment.

An integrative network reveals a potential miRNA-RBP-splicing regulatory axis

Our preceding analyses showed RSV infection concurrently alters host miRNA, RBP, and AS landscapes. We constructed a multi-layered regulatory network to integrate these findings. Co-expression analysis of 87 conserved differentially expressed RBPs and 94 RAS events identified 4 core RBP genes (*SAMD4A*, *ENOX1*, *ZFP36*, *YBX2*) strongly correlated with 26 RAS events (Figure 4A). These core RBPs exhibited distinct expression trends: *SAMD4A*, *ENOX1*, and *ZFP36* were progressively upregulated during infection, while *YBX2* was downregulated (Figure 4C), and their targeted 26 RAS genes were enriched in endocytosis and EGFR signaling pathways (Figure 4B). Integrating miRNA data to identify upstream regulators uncovered a regulatory cascade involving the let-7 miRNA family and RBPs *SAMD4A/ENOX1* (Figure 4A). RSV infection downregulated let-7 family members (e.g., let-7a-3p, let-7b-3p, let-7f-1-3p, let-7f-2-3p; Figure 4D), de-repressing their predicted targets *SAMD4A* and *ENOX1* (concomitantly upregulated). This upregulation correlated with splicing changes in viral replication-related host genes (e.g., *TNIP1*, *NR5A2*).

Taken together, our integrative analysis identifies a putative post-transcriptional regulatory axis (Figure 5) underlying RSV infection: downregulation of let-7 family miRNAs (e.g., let-7f-2-3p, let-7a-3p) correlates with the upregulation of RBPs *SAMD4A* and *ENOX1*, and these RBPs in turn show strong associations with AS of key host genes (e.g., *TNIP1*, *NR5A2*) involved in viral replication and immunity. This cascade may collectively shape a cellular environment conducive to the life cycle of RSV.

Discussion

This study integrated multi-omics data of RSV-infected A549 cells from the GEO database and employed bioinformatics methods to construct a miRNA-RBP-AS regulatory network, which for the first time identified the potential let-7-SAMD4A/ENOX1-TNIP1/NR5A2 axis.

Analysis of miRNA-seq data reveals that RSV infection dramatically remodels the host miRNA expression profile, a finding consistent with previous literature showing that RSV manipulates cellular miRNAs to facilitate immune evasion and replication [36]. This includes the modulation of specific miRNAs like the let-7 family, which directly impacts viral replication, and can generate a unique miRNA "fingerprint" that may reflect disease severity [37]. A key insight from our study comes from the functional analysis of these dysregulated miRNAs, whose predicted target genes were significantly enriched in the *Wnt* signaling pathway. The *Wnt* signaling pathway is fundamentally important for lung epithelial stem cell function and differentiation. Notably, parallels can be drawn to influenza virus, which downregulates the *Wnt* pathway, thereby impairing host lung repair [38]. Furthermore, influenza virus can manipulate the *Wnt/β-catenin* signaling cascade to directly influence its own mRNA levels and viral production [39]. Our findings, therefore, strongly suggest that a similar mechanism may exist during RSV infection, positioning the *Wnt* pathway as a critical nexus where miRNA-mediated dysregulation could simultaneously impact host immune responses and viral replication efficiency.

Building on the miRNA-driven changes, analysis of RNA-seq datasets further reinforces the central role of host RBPs—master regulators of RNA fate—in RSV pathogenesis, revealing a dynamic and robust reprogramming of these factors following infection. The cohort of upregulated RBPs was overwhelmingly enriched in antiviral functions, including direct responses to viral infection and negative regulation of the viral life cycle. This potent antiviral signature was

Figure 5. Schematic representation of the proposed regulatory network during RSV infection.

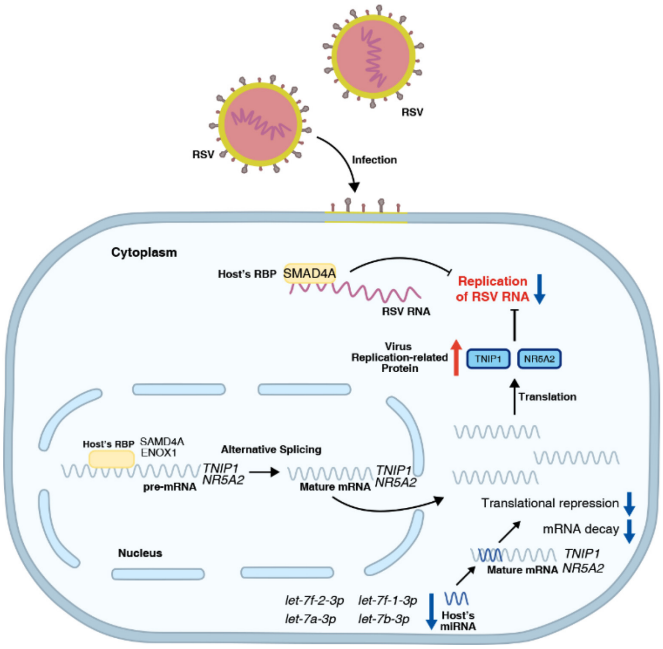

exemplified by the strong, time-dependent induction of several ISGs that function as RBPs. The established functions of these specific ISGs in other viral contexts highlight their potential potency against RSV [40]. *IFI16*, for instance, can directly sense viral RNA to amplify the RIG-I pathway during influenza infection [41], while *IFIT1* acts as a direct inhibitor by recognizing the 5'-triphosphate ends of viral RNA [42]. Others, like *IFIT5* and *ISG20*, contribute by either enhancing interferon signaling or directly degrading viral RNA of pathogens like hepatitis B virus (HBV) [43–45]. However, despite their established roles as broad-spectrum antiviral factors, their precise mechanisms and contributions during RSV infection remain to be elucidated—our study fills this knowledge gap by delineating their potential involvement in the regulation of host AS.

We constructed a miRNA-RBP-AS regulatory axis to integrate these observations into a cohesive framework, and propose it as a mechanistic hypothesis for the key AS changes observed during RSV infection. This axis centers on two core RBP genes—*SAMD4A* and *ENOX1*—whose expression levels show strong correlation with the AS of host factors like *TNIP1* and *NR5A2*. This association is particularly compelling given *TNIP1*'s clinical relevance: its genetic polymorphisms are linked to the severity of RSV-induced bronchiolitis in infants [46]. While *TNIP1* is known to inhibit other viruses (e.g., human immunodeficiency virus, HIV) [47], the impact of its specific splice isoforms has been unknown; our study fills this gap by identifying a novel, longer *TNIP1* isoform that was preferentially produced upon RSV infection, providing a tangible molecular event for future investigation. *NR5A2* encodes a nuclear receptor transcription factor that binds to the DNA sequence 5'-TCAAGGCCA-3' to regulate gene expression. Studies have shown that NR5A2 can inhibit pancreatic inflammatory responses by binding to the promoter regions of inflammatory genes [48]. Given this anti-inflammatory role, we hypothesize *NR5A2* may also be involved in tuning host immune responses during RSV infection, with its AS changes potentially modifying this regulatory function.

Further analysis strengthens the validity of this miRNA-RBP-AS axis by linking the upregulation of *SAMD4A* and *ENOX1* to the downregulation of their predicted upstream regulators: members of the let-7 miRNA family. This inverse relationship supports a classic de-repression mechanism. Studies have shown let-7 family members inhibit viral replication through dual mechanisms—directly targeting viral genomes (e.g., hepatitis C virus (HCV) NS5B) and activating host innate immunity via the *JAK/STAT* and *RIG-I* pathways [49,50]. The biological context for these RBPs is also intriguing. *SAMD4A*, for instance, is a known antiviral factor that can inhibit HBV replication by directly binding its RNA [51], suggesting RSV may induce a broad antiviral player that is then co-opted to modulate splicing. The role of the other core RBP, *ENOX1*, in viral pathogenesis is novel and warrants further exploration. Together, these findings construct a compelling narrative (Figure 5): RSV-induced suppression of let-7 family miRNAs may de-repress *SAMD4A* and *ENOX1*, which in turn modulate the splicing of key host factors like *TNIP1* and the inflammation-related gene *NR5A2* [48], thereby fine-tuning the cellular environment to balance viral replication and host immunity.

While this study provides a comprehensive computational framework, several limitations should be acknowledged to contextualize the findings. First, the proposed regulatory network is based on bioinformatic analysis of correlations and predictions. Direct experimental validation—such as luciferase assays to confirm miRNA-target interactions and functional studies to assess the impact of specific RBPs and splice isoforms—is essential to definitively establish the causal relationships and molecular mechanisms. Second, our findings are derived exclusively from the A549 cell line, and the rationale for this selection requires clarification. A549 cells are derived from human type II alveolar epithelial cells, sharing consistency in origin with one of the primary target cells of RSV infection—this ensures the cellular model aligns with the physiological target of RSV in the lower respiratory tract. Moreover, A549 cells have been widely used in RSV infection mechanism research, with their transcriptomic profiles and viral infection models fully characterized in existing literature [52,53]. This extensive prior validation not only guarantees the reliability of our experimental background but also enables direct comparability between our findings and previous RSV-related studies, laying a solid foundation for the initial discovery of post-transcriptional regulatory networks. However, as a transformed adenocarcinoma cell line, A549 cells lack the phenotypic diversity of primary respiratory epithelial cells and cannot recapitulate in vivo cellular crosstalk, which may bias the identified miRNA-RBP-AS interactions. Additionally, the absence of clinical sample validation limits the translational relevance of our findings. These limitations, however, also define clear and compelling directions for follow-up studies

aimed at validating and expanding upon the foundational network established here.

To address these outlined limitations, we propose targeted follow-up experiments to validate and extend the miRNA-RBP-AS regulatory axis. First, luciferase reporter assays will be performed in A549 cells to confirm the predicted direct interactions between let-7 family miRNAs and the 3'-UTRs of *SAMD4A* and *ENOX1*. Second, functional validation of RBPs will be conducted in A549 cells via siRNA-mediated knockdown or plasmid-based overexpression of *SAMD4A* and *ENOX1*, followed by RNA-seq to systematically quantify AS changes, and isoform-specific qPCR to verify the altered splicing patterns of *TNIP1* and *NR5A2*. Additionally, qPCR and Western blot will be used to assess downstream inflammatory and antiviral gene expression. Third, primary cell validation will use human bronchial epithelial cells (HBECs) and primary macrophages to recapitulate the in vivo respiratory microenvironment, with RSV infection to confirm whether the regulatory axis is conserved beyond adenocarcinoma cell lines. Finally, clinical sample correlation will involve analyzing the expression levels of key miRNAs, RBPs, and splice isoforms in nasal swabs or bronchoalveolar lavage fluid from RSV-infected infants, correlating these molecular signatures with clinical disease severity scores to evaluate their potential as diagnostic or prognostic biomarkers.

Conclusions

This work provides a comprehensive, systems-level view of the post-transcriptional regulatory landscape during RSV infection, derived primarily from bioinformatic analyses. We have predicted a potential regulatory cascade where RSV may hijack the host's miRNA, RBP, and AS machinery to its own benefit—with the identified let-7-*SAMD4A/ENOX1*-*TNIP1/NR5A2* axis emerging as a prime candidate for future mechanistic investigation. While these findings lay a foundational framework for understanding post-transcriptional regulation in RSV infection, they remain speculative and require rigorous in vitro and in vivo validation to confirm causal relationships, functional relevance, and potential translational value as a nexus of novel targets for RSV antiviral therapeutic intervention.

Acknowledgements

We are very grateful to Dr. Junru Qin and Zidong Zhang of the Center for BioBigData Analysis, Biosalt Inc.for their support and help in data analysis.

Corresponding author

Shuangshuang Li, M. Med.
Department of Pediatrics, Chinese PLA General Hospital of Central Theater Command,
Wuhan, 430070, Hubei Province, China
Tel: +86 18064082539
Fax: +86 027-50772077
Email: 18064082539@163.com

Conflict of interest

No conflict of interest is declared.

References

1. Agac A, Kolbe SM, Ludlow M, Osterhaus A, Meineke R, Rimmelzwaan GF (2023) Host responses to respiratory syncytial virus infection. Viruses 15: 1999. doi: 10.3390/v15101999.
2. Feng Q, Feng Z, Yang B, Han S, Wen S, Lu G, Jin R, Xu B, Zhang H (2023) Metatranscriptome reveals specific immune and microbial signatures of respiratory syncytial virus infection in children. Microbiol Spectr 11: e0410722. doi: 10.1128/spectrum.04107-22.
3. Duan Y, Liu Z, Zang N, Cong B, Shi Y, Xu L, Jiang M, Wang P, Zou J, Zhang H, Feng Z, Feng L, Ren L, Liu E, Li Y, Zhang Y, Xie Z (2024) Landscape of respiratory syncytial virus. Chin Med J (Engl) 137: 2953–2978. doi: 10.1097/CM9.0000000000003354.
4. Ule J, Blencowe BJ (2019) Alternative splicing regulatory networks: functions, mechanisms, and evolution. Mol Cell 76: 329–345. doi: 10.1016/j.molcel.2019.09.017.
5. Garcia-Moreno M, Järvelin AI, Castello A (2018) Unconventional RNA-binding proteins step into the virus-host battlefront. Wiley Interdiscip Rev RNA 9: e1498. doi: 10.1002/wrna.1498.
6. Li MM, MacDonald MR, Rice CM (2015) To translate, or not to translate: viral and host mRNA regulation by interferon-stimulated genes. Trends Cell Biol 25: 320–329. doi: 10.1016/j.tcb.2015.02.001.
7. Sehrawat S, Garcia-Blanco MA (2023) RNA virus infections and their effect on host alternative splicing. Antiviral Res 210: 105503. doi: 10.1016/j.antiviral.2022.105503.
8. Mann JT, Riley BA, Baker SF (2023) All differential on the splicing front: host alternative splicing alters the landscape of virus-host conflict. Semin Cell Dev Biol 146: 40–56. doi: 10.1016/j.semcdb.2023.01.013.
9. Liao KC, Garcia-Blanco MA (2021) Role of alternative splicing in regulating host response to viral infection. Cells 10: 1720. doi: 10.3390/cells10071720.
10. Liu P, Lu M, Tian B, Li K, Garofalo RP, Prusak D, Wood TG, Brasier AR (2009) Expression of an *IKKgamma* splice variant determines *IRF3* and canonical *NF-kappaB* pathway utilization in ssRNA virus infection. PLoS One 4: e8079. doi: 10.1371/journal.pone.0008079.
11. Lindquist ME, Lifland AW, Utley TJ, Santangelo PJ, Crowe JE, Jr. (2010) Respiratory syncytial virus induces host RNA

stress granules to facilitate viral replication. J Virol 84: 12274–12284. doi: 10.1128/JVI.00260-10.
12. Bartel DP (2009) MicroRNAs: target recognition and regulatory functions. Cell 136: 215–233. doi: 10.1016/j.cell.2009.01.002.
13. Rossi GA, Silvestri M, Colin AA (2015) Respiratory syncytial virus infection of airway cells: role of microRNAs. Pediatr Pulmonol 50: 727–732. doi: 10.1002/ppul.23193.
14. Bakre A, Wu W, Hiscox J, Spann K, Teng MN, Tripp RA (2015) Human respiratory syncytial virus non-structural protein NS1 modifies miR-24 expression via transforming growth factor-β. J Gen Virol 96: 3179–3191. doi: 10.1099/jgv.0.000261.
15. Chen S, Zhou Y, Chen Y, Gu J (2018) fastp: an ultra-fast all-in-one FASTQ preprocessor. Bioinformatics 34: i884–i890. doi: 10.1093/bioinformatics/bty560.
16. Love MI, Huber W, Anders S (2014) Moderated estimation of fold change and dispersion for RNA-seq data with DESeq2. Genome Biol 15: 550. doi: 10.1186/s13059-014-0550-8.
17. Castello A, Fischer B, Eichelbaum K, Horos R, Beckmann BM, Strein C, Davey NE, Humphreys DT, Preiss T, Steinmetz LM, Krijgsveld J, Hentze MW (2012) Insights into RNA biology from an atlas of mammalian mRNA-binding proteins. Cell 149: 1393–1406. doi: 10.1016/j.cell.2012.04.031.
18. Castello A, Fischer B, Frese CK, Horos R, Alleaume AM, Foehr S, Curk T, Krijgsveld J, Hentze MW (2016) Comprehensive identification of RNA-binding domains in human cells. Mol Cell 63: 696–710. doi: 10.1016/j.molcel.2016.06.029.
19. Gerstberger S, Hafner M, Tuschl T (2014) A census of human RNA-binding proteins. Nat Rev Genet 15: 829–845. doi: 10.1038/nrg3813.
20. Hentze MW, Castello A, Schwarzl T, Preiss T (2018) A brave new world of RNA-binding proteins. Nat Rev Mol Cell Biol 19: 327–341. doi: 10.1038/nrm.2017.130.
21. Cheng C, Liu L, Bao Y, Yi J, Quan W, Xue Y, Sun L, Zhang Y (2021) SUVA: splicing site usage variation analysis from RNA-seq data reveals highly conserved complex splicing biomarkers in liver cancer. RNA Biol 2021: 1–15. doi: 10.1080/15476286.2021.1940037.
22. Xiao F, Zuo Z, Cai G, Kang S, Gao X, Li T (2009) miRecords: an integrated resource for microRNA-target interactions. Nucleic Acids Res 37: D105–110. doi: 10.1093/nar/gkn851.
23. Hsu SD, Lin FM, Wu WY, Liang C, Huang WC, Chan WL, Tsai WT, Chen GZ, Lee CJ, Chiu CM, Chien CH, Wu MC, Huang CY, Tsou AP, Huang HD (2011) miRTarBase: a database curates experimentally validated microRNA-target interactions. Nucleic Acids Res 39: D163–169. doi: 10.1093/nar/gkq1107.
24. Skoufos G, Kakoulidis P, Tastsoglou S, Zacharopoulou E, Kotsira V, Miliotis M, Mavromati G, Grigoriadis D, Zioga M, Velli A, Koutou I, Karagkouni D, Stavropoulos S, Kardaras FS, Lifousi A, Vavalou E, Ovsepian A, Skoulakis A, Tasoulis SK, Georgakopoulos SV, Plagianakos VP, Hatzigeorgiou AG (2024) TarBase-v9.0 extends experimentally supported miRNA-gene interactions to cell-types and virally encoded miRNAs. Nucleic Acids Res 52: D304–D310. doi: 10.1093/nar/gkad1071.
25. Chen Y, Wang X (2020) miRDB: an online database for prediction of functional microRNA targets. Nucleic Acids Res 48: D127–D131. doi: 10.1093/nar/gkz757.
26. Tastsoglou S, Alexiou A, Karagkouni D, Skoufos G, Zacharopoulou E, Hatzigeorgiou AG (2023) DIANA-microT 2023: including predicted targets of virally encoded miRNAs. Nucleic Acids Res 51: W148–W153. doi: 10.1093/nar/gkad283.
27. Betel D, Koppal A, Agius P, Sander C, Leslie C (2010) Comprehensive modeling of microRNA targets predicts functional non-conserved and non-canonical sites. Genome Biol 11: R90. doi: 10.1186/gb-2010-11-8-r90.
28. Krek A, Grün D, Poy MN, Wolf R, Rosenberg L, Epstein EJ, MacMenamin P, da Piedade I, Gunsalus KC, Stoffel M, Rajewsky N (2005) Combinatorial microRNA target predictions. Nat Genet 37: 495–500. doi: 10.1038/ng1536.
29. McGeary SE, Lin KS, Shi CY, Pham TM, Bisaria N, Kelley GM (2019) The biochemical basis of microRNA targeting efficacy. Science 366: eaav1741. doi: 10.1126/science.aav1741.
30. Kertesz M, Iovino N, Unnerstall U, Gaul U, Segal E (2007) The role of site accessibility in microRNA target recognition. Nat Genet 39: 1278–1284. doi: 10.1038/ng2135.
31. Gaidatzis D, van Nimwegen E, Hausser J, Zavolan M (2007) Inference of miRNA targets using evolutionary conservation and pathway analysis. BMC Bioinformatics 8: 69. doi: 10.1186/1471-2105-8-69.
32. Griffiths-Jones S, Saini HK, van Dongen S, Enright AJ (2008) miRBase: tools for microRNA genomics. Nucleic Acids Res 36: D154–158. doi: 10.1093/nar/gkm952.
33. Wu T, Hu E, Xu S, Chen M, Guo P, Dai Z, Feng T, Zhou L, Tang W, Zhan L, Fu X, Liu S, Bo X, Yu G (2021) clusterProfiler 4.0: a universal enrichment tool for interpreting omics data. Innovation 2: 100141. doi: 10.1016/j.xinn.2021.100141.
34. Kassambara A, Mundt F (2020). factoextra: extract and visualize the results of multivariate data analyses. R package version 1.0.7.999. Available: https://github.com/kassambara/factoextra. Accessed: 19 July 2025.
35. Kolde R (2025). pheatmap: pretty heatmaps. R package version 1.0.13. Available: https://CRAN.R-project.org/package=pheatmap. Accessed: 19 July 2025.
36. Thornburg NJ, Hayward SL, Crowe JE, Jr (2012) Respiratory syncytial virus regulates human microRNAs by using mechanisms involving beta interferon and NF-κB. mBio 3: e00220–12. doi: 10.1128/mBio.00220-12.
37. Bakre A, Mitchell P, Coleman JK, Jones LP, Saavedra G, Teng M, Tompkins SM, Tripp RA (2012) Respiratory syncytial virus modifies microRNAs regulating host genes that affect virus replication. J Gen Virol 93: 2346–2356. doi: 10.1099/vir.0.044255-0.
38. Hancock AS, Stairiker CJ, Boesteanu AC, Monzón-Casanova E, Lukasiak S, Mueller YM, Stubbs AP, García-Sastre A, Turner M, Katsikis PD (2018) Transcriptome analysis of infected and bystander type 2 alveolar epithelial cells during influenza A virus infection reveals in vivo Wnt pathway downregulation. J Virol 92: e01325–18. doi: 10.1128/JVI.01325-18.
39. More S, Yang X, Zhu Z, Bamunuarachchi G, Guo Y, Huang C, Bailey K, Metcalf JP, Liu L (2018) Regulation of influenza virus replication by *Wnt/β-catenin* signaling. PLoS One 13: e0191010. doi: 10.1371/journal.pone.0191010.
40. Bouillier C, Cosentino G, Léger T, Rincheval V, Richard CA, Desquesnes A, Sitterlin D, Blouquit-Laye S, Eléouët JF, Gault E, Rameix-Welti MA (2019) The interactome analysis of the respiratory syncytial virus protein M2-1 suggests a new role in

viral mRNA metabolism post-transcription. Sci Rep 9: 15258. doi: 10.1038/s41598-019-51746-0.
41. Jiang Z, Wei F, Zhang Y, Wang T, Gao W, Yu S, Wang M, Tong Q, Gao C, Chang KC, Liu J (2021) IFI16 directly senses viral RNA and enhances *RIG-I* transcription and activation to restrict influenza virus infection. Nat Microbiol 6: 932–945. doi: 10.1038/s41564-021-00907-x.
42. Pichlmair A, Lassnig C, Eberle CA, Górna MW, Baumann CL, Burkard TR, Bürckstümmer T, Stefanovic A, Krieger S, Bennett KL, Rülicke T, Weber F, Colinge J, Müller M, Superti-Furga G (2011) IFIT1 is an antiviral protein that recognizes 5'-triphosphate RNA. Nat Immunol 12: 624–630. doi: 10.1038/ni.2048.
43. Meischel T, Fritzlar S, Villalon-Letelier F, Tessema MB, Brooks AG, Reading PC, Londrigan SL (2021) IFITM proteins that restrict the early stages of respiratory virus infection do not influence late-stage replication. J Virol 95: e0083721. doi: 10.1128/JVI.00837-21.
44. Zhang B, Liu X, Chen W, Chen L (2013) IFIT5 potentiates anti-viral response through enhancing innate immune signaling pathways. Acta Biochim Biophys Sin (Shanghai) 45: 867–874. doi: 10.1093/abbs/gmt088.
45. Liu Y, Nie H, Mao R, Mitra B, Cai D, Yan R, Guo JT, Block TM, Mechti N, Guo H (2017) Interferon-inducible ribonuclease ISG20 inhibits hepatitis B virus replication through directly binding to the epsilon stem-loop structure of viral RNA. PLoS Pathog 13: e1006296. doi: 10.1371/journal.ppat.1006296.
46. Martin-Vicente M, Mthiyane H, Jiménez-Sousa MA, Subramoney K, Hellferscee O, Wolter N, Walaza S, Fernández-Rodríguez A, Cohen C, von Gottberg A, Resino S, Martínez I, Treurnicht FK (2023) TNFAIP3-interacting protein 1 polymorphisms and their association with symptomatic human respiratory syncytial virus infection and bronchiolitis in infants younger than one year from South Africa: a case-control study. Int J Infect Dis 136:107–110. doi: 10.1016/j.ijid.2023.09.013.
47. Ramirez VP, Gurevich I, Aneskievich BJ (2012) Emerging roles for TNIP1 in regulating post-receptor signaling. Cytokine Growth Factor Rev 23: 109–118. doi: 10.1016/j.cytogfr.2012.04.002.
48. Cobo I, Martinelli P, Flández M, Bakiri L, Zhang M, Carrillo-de-Santa-Pau E, Jia J, Sánchez-Arévalo Lobo V, Megías D, Felipe I, Del Pozo N, Millán I, Thommesen L, Bruland T, Olson SH, Smith J, Schoonjans K, Bamlet WR, Petersen GM, Malats N, Amundadottir LT, Wagner EF, Real FX (2018) Transcriptional regulation by *NR5A2* links differentiation and inflammation in the pancreas. Nature 554: 533–557. doi: 10.1038/nature25751.
49. Letafati A, Najafi S, Mottahedi M, Karimzadeh M, Shahini A, Garousi S, Abbasi-Kolli M, Sadri Nahand J, Tamehri Zadeh SS, Hamblin MR, Rahimian N, Taghizadieh M, Mirzaei H (2022) MicroRNA *let-7* and viral infections: focus on mechanisms of action. Cell Mol Biol Lett 27: 14. doi: 10.1186/s11658-022-00317-9.
50. Yeh YJ, Tseng CP, Hsu SD, Huang HY, Lai MMC, Huang HD, Cheng JC (2021) Dual effects of *Let-7b* in the early stage of hepatitis C virus infection. J Virol 95: e01800–20. doi: 10.1128/JVI.01800-20.
51. Wang Y, Fan X, Song Y, Liu Y, Liu R, Wu J, Li X, Yuan Q, Fu G, Xia N, Han J (2021) *SAMD4* family members suppress human hepatitis B virus by directly binding to the Smaug recognition region of viral RNA. Cell Mol Immunol 18: 1032–1044. doi: 10.1038/s41423-020-0431-x.
52. Rajan A, Piedra FA, Aideyan L, McBride T, Robertson M, Johnson HL, Aloisio GM, Henke D, Coarfa C, Stossi F, Menon VK, Doddapaneni H, Muzny DM, Javornik Cregeen SJ, Hoffman KL, Petrosino J, Gibbs RA, Avadhanula V, Piedra PA (2022) Multiple respiratory syncytial virus (RSV) strains infecting HEp-2 and A549 cells reveal cell line-dependent differences in resistance to RSV infection. J Virol 96: e0190421. doi: 10.1128/jvi.01904-21.
53. Vanetti C, Saulle I, Artusa V, Moscheni C, Cappelletti G, Zecchini S, Strizzi S, Garziano M, Fenizia C, Tosoni A, Broggiato M, Ogno P, Nebuloni M, Clerici M, Trabattoni D, Limanaqi F, Biasin M (2024) A complex remodeling of cellular homeostasis distinguishes RSV/SARS-CoV-2 co-infected A549-hACE2 expressing cell lines. Microb Cell 11: 353–367. doi: 10.15698/mic2024.10.838.

Annex – Supplementary Items

Supplementary Figure 1. Differential gene expression analysis in the GSE231788 and GSE155151 datasets.

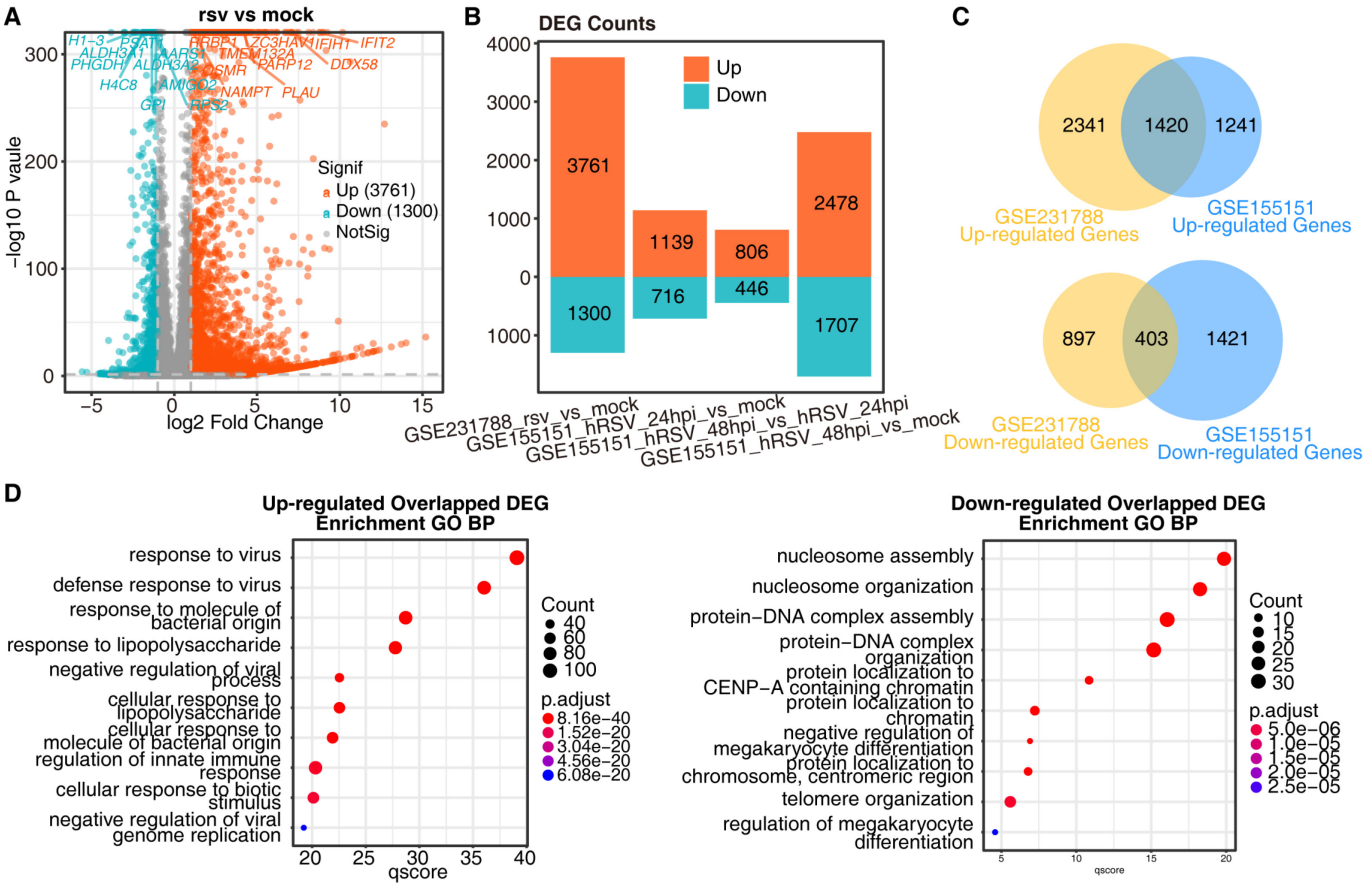

A. Volcano plot depicting differentially expressed genes (DEGs) in the GSE231788 dataset (DESeq2; FoldChange ≥ 1.5 or FoldChange ≤ 0.66, FDR ≤ 0.05); **B.** Bar plot summarizing the number of DEGs identified across different group comparisons; **C.** Venn diagram illustrating the overlap of conserved DEGs between the GSE231788 and GSE155151 datasets; **D.** GO enrichment analysis of the conserved DEGs.

Supplementary Figure 2. AS analysis in the GSE155151 dataset.

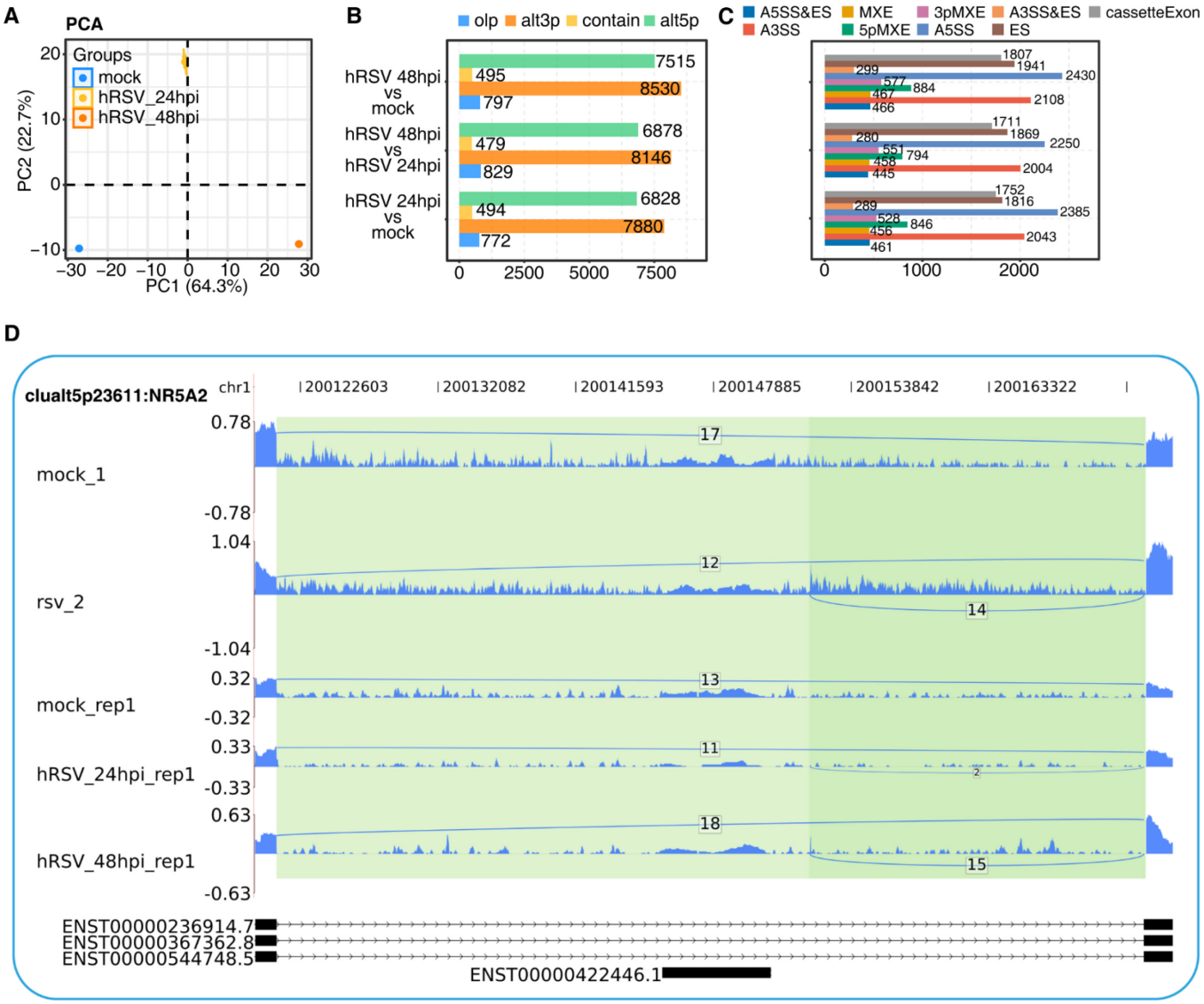

A. PCA based on the proportions of AS events in the GSE155151 dataset; **B.** Bar plot presenting the number of AS event types identified by SUVA in the GSE155151 dataset; **C.** Bar plot illustrating the number of SUVA-detected splicing events annotated to canonical AS event types; D. Visualization of read alignments and quantification of AS events clualt5p23611 in NR5A2.

Supplementary Figure 3. AS analysis in the GSE155151 dataset.

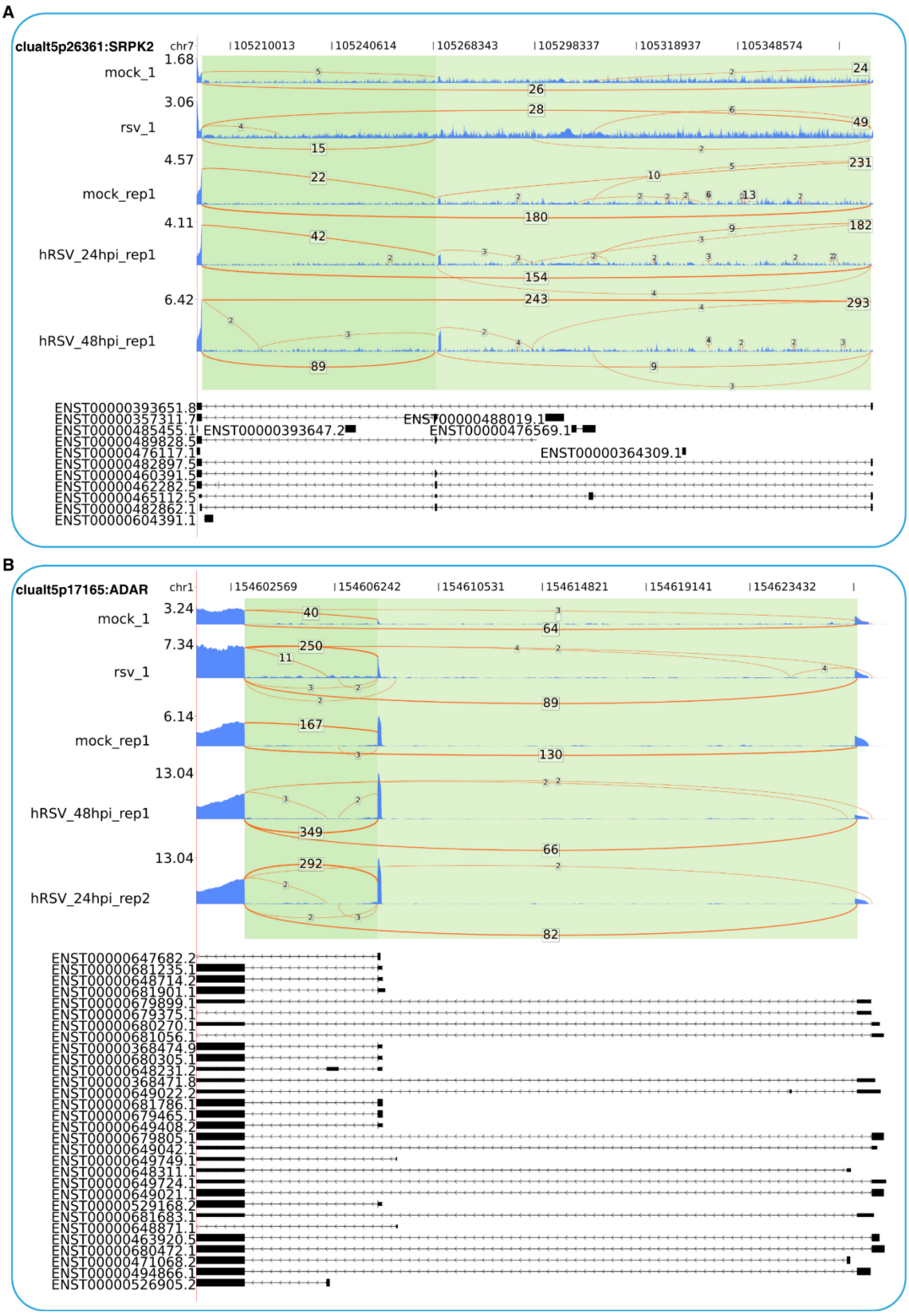

A-B. Visualization of read alignments and quantification of AS events clualt5p26361 in SRPK2, and clualt5p17165 in ADAR.